Influence of aging on electrolytic capacitors function in static converters: Fault prediction method

Pascal Venet, Amine Lahyani, Guy Grellet, A. Ah-Jaco

Eur. Phys. J. AP 5, 71–83 (1999)

THE EUROPEAN PHYSICAL JOURNAL APPLIED PHYSICS

Influence of aging on electrolytic capacitors function in static converters: Fault prediction method

P. Venet[a], A. Lahyani, G. Grellet, and A. Ah-Jaco

CEGELY, Université Claude Bernard de Lyon[b], bâtiment 721, 43 boulevard du 11 Novembre 1918, 69622 Villeurbanne Cedex, France

Received: 20 March 1998 / Revised: 14 September 1998 / Accepted: 9 October 1998

Abstract. The failure of electrolytic capacitors is the cause of most breakdowns of static converters. The function of these capacitors is to filter and to store electrical energy. Accelerated aging tests showed that the increase of the internal resistance ESR of the capacitors is a good indicator of their faulty state. The filter function is affected by the capacitors wearout on the one hand. At high frequency, the voltage ripple at the terminals of the capacitors increases according to ESR rise. On the other hand, the storage function is not much influenced by the capacitors aging. As static converters work most of the time at variable load, high transient values of the voltage ripple occur when output current changes that can induce false alarms. These transients are verified theoretically and experimentally. In order to avoid these transients effects, we suggest to monitor the fundamental component of the voltage ripple. This latter waveform is the best signature of the capacitors state. The ESR of the capacitors and the time before their failure are deduced from the processing of this waveform with other converter parameters such as input voltage, output current and ambient temperature.

PACS. 84.30.Jc Power electronics; power supply circuits – 84.32.Tt Capacitors – 84.37.+q Electric variable measurements (including voltage, current, resistance, capacitance, inductance, impedance, and admittance, etc.)

1 Introduction

About 30% of breakdowns of electronic equipment are caused by static converters which represent essential subsystems for such devices. Since more than half of faults of static converters are due to electrolytic capacitors [1,2], the monitoring of these passive components is necessary.

To avoid the risks caused by the failure of the capacitors, and in order to establish an efficient prevention against sudden stoppages, a predictive maintenance method is applied to the static converters.

The main functions of the electrolytic capacitors (filter and storage of electrical energy) are similar in a great majority of converters.

Thus, this method is presented for capacitors used in two types of static converters (AC/DC and DC/DC switching mode power supplies provided by static converters manufacturer).

After a presentation of the converters taken in example, we analyze the influence of thermal aging on the electrolytic capacitors. The equivalent series resistance (ESR) is a good indicator of their faults and its evolution *versus* aging time and temperature fits a well known law.

Then, we study how the aging of input and output capacitors affects the capability of the latter to filter and store electrical energy. We demonstrate that the voltage ripple applied to the capacitors varies almost proportionally to the ESR [1].

To monitor the increase of ESR, some authors [3,4] suggest to use the rectified average signal of the voltage ripple as an image of the latter. As static converters usually work at variable load, we verify theoretically and experimentally that high transient values of the voltage ripple are generated by the load variation. These transients may lead to wrong predicted lifetimes of the capacitors.

To get rid of these transient values and have a better image of ESR, we suggest to extract the fundamental component of the voltage ripple.

We established a method to predict the fault of electrolytic capacitors. Since the input and the output voltages ripple does not depend only on ESR, but also on the output current I_o, the input voltage V_i and the ambient temperature T_a, all these parameters are taken into account for the monitoring of the capacitors.

Software and electronic modules have been developed to compute online the lifetime of the electrolytic capacitors.

Finally, we present the results obtained by the prototype.

[a] e-mail: venet@cegely.univ-lyon1.fr

[b] UPRES A 5005 CNRS

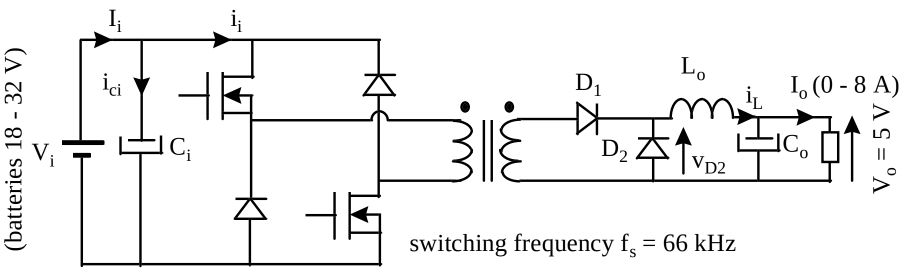

Fig. 1. Diagram of the converter SC1.

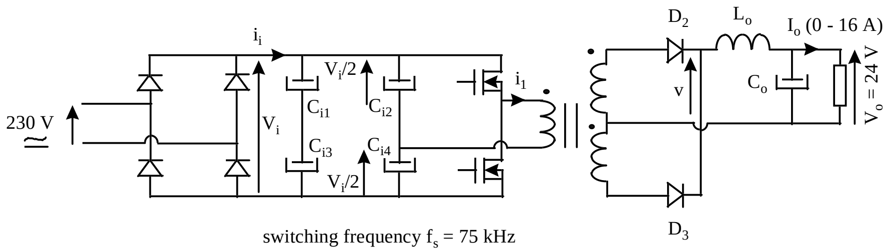

Fig. 2. Diagram of the converter SC2.

2 Presentation of the converters

The first static converter (SC1) studied is an industrial DC/DC "Forward" half-bridge asymmetrical switching mode power supply (40 W) as shown in Figure 1.

- The output filtering capacitors symbolized C_o are 2 aluminum electrolytic capacitors rated 2 200 μF, 10 V, 105 ℃, (MARCON CE USM 1A 222) in parallel.
- The input filtering capacitors symbolized C_i are 3 capacitors rated 1 500 μF, 35 V, 105 ℃, (NIPPON CHEMI-CON SXE 35VB-1500 18X20) in parallel with 2 capacitors rated 3 300 μF, 35 V, 105 ℃, (NIPPON CHEMI-CON SXE 35VB-3300 18X40). For converter compactness reason, two types of capacitors are used.

The second converter (SC2) is an industrial AC/DC "Forward" half-bridge symmetrical switching mode power supply (384 W) as shown in Figure 2.

- The output filtering capacitors symbolized C_o are 2 aluminum electrolytic capacitors rated 1 500 μF, 35 V, 105 ℃, (NIPPON CHEMI-CON SXE 35VB-1500 18X20) in parallel.
- The input filtering capacitors symbolized C_i are 4 aluminum electrolytic capacitors rated 680 μF, 200 V, 105 ℃, (NIPPON CHEMI-CON KMH 200VNSN-680 25.4X40).

In the converters SC1 and SC2, the electrolytic capacitors are used to filter and to store the electrical energy. For these converters, industrial users require that the capacitors must hold the same power level during at least 20 milliseconds, when the input voltage drops.

At ambient temperature equal to 25 ℃, the electrolytic capacitors are responsible in SC1 and SC2 for more than 50% of breakdowns accounted to the power components.

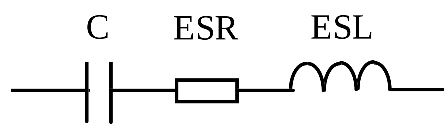

Fig. 3. Simplified equivalent circuit of an electrolytic capacitor.

3 Determination of the main parameters of the aged capacitors

3.1 Equations and equivalent circuits

An electrolytic capacitor can be schematized by the equivalent circuit in Figure 3, where:

- C: Capacitance (frequency dependent);
- ESR: Equivalent series resistance representing all ohmic losses in the capacitor (frequency dependent);
- ESL: Equivalent series inductance. Its value near some nH is frequency independent.

To study the aging of these components, we take for example the capacitors rated 2 200 μF, 10 V, 105 ℃, used to filter the output voltage of the converter SC1.

The different parameters characterizing the capacitors are measured with the help of a LCR meter in a frequency range of [20 Hz–1 MHz].

The measurement equipment shows that the capacitor is equivalent to a resistance R_s in series with a capacitance C_s until the frequency f_r ($\approx$ 100 kHz) is reached:

$$f_r = 1/\left(2\pi\sqrt{ESLC}\right). \quad (1)$$

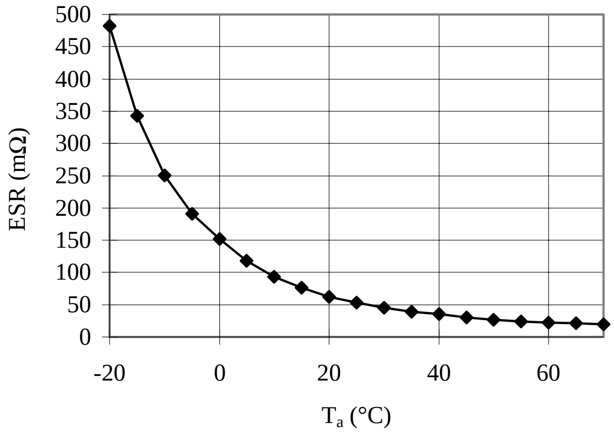

Fig. 4. *ESR versus* ambient temperature for sound capacitors measured at 66 kHz.

By considering the simplified equivalent circuit of a capacitor and by identifying its impedance to the measured impedance we get:

$$C_s = \frac{C}{1 - ESLC\omega^2} \tag{2}$$

$$R_s = ESR. \tag{3}$$

3.2 Influence of the ambient temperature

The increase of the ambient temperature T_a leads to a rise of C_s and a decrease of $R_s = ESR$. The influence of T_a on ESR, measured at the switching frequency of SC1 *i.e.* 66 kHz, is shown in Figure 4.

To measure ESR, the LCR meter injects a low current ripple through the capacitor. The temperature of the capacitor T_c can then be assimilated to the environmental temperature T_a because the self heating can be neglected.

3.3 Influence of the current ripple across the capacitors

Actually, during operation of the converter SC1, the current ripple can not be neglected. The case temperature T_c is thus equal to the sum of T_a and a temperature difference ΔT due to Joule losses in the capacitor:

$$T_c = T_a + \Delta T. \tag{4}$$

The difference ΔT depends on ESR, on the current across the capacitor and on the thermal resistance between the case and the ambient, as shown by the relation (5) [7–9]:

$$\Delta T = \frac{ESRI^2}{HS} = \frac{P}{HS} \tag{5}$$

with: I: RMS value of the current ripple; H: heat transfer per unit surface area (W/K m^2). H depends on the diameter of the package, the diameter of the roll and on the cooling conditions [7,8]; S: surface area of the capacitor.

3.4 Aging tests

In order to observe the evolution of ESR and C_s *versus* aging time and temperature, we applied to lots of 50 capacitors used in the converters SC1 and SC2, an accelerated thermal aging under their nominal voltages and temperature ($T = 105$ °C).

In Figure 5, we represent the variation of ESR and C_s measured *versus* frequency for sound capacitors rated 2 200 μF, 10 V, 105 °C and after an aging test of 3640 hours.

The loss of electrolyte inside the capacitor leads to a decrease of the capacitance C_s and an increase of the resistance ESR [3,8]. In addition, since the inductance ESL is independent on the aging, the resonance frequency rises (*cf.* Eqs. (1) and (2)).

The increase of ESR *versus* aging time is interesting because at the switching frequency of the converter, $1/(C\cdot\omega)$ and $ESL\cdot\omega$ can be neglected compared to ESR. Therefore, at this frequency, the capacitor impedance is almost equal to ESR. This evolution is also important since it determines the internal heating of the capacitor and then its lifetime [10,11].

The rise of ESR *versus* the aging is more important than the decrease of C_s. It represents a good indicator of fault of electrolytic capacitors, more especially as a theoretical law to predict ESR can be determined.

In Figure 6, we represent the experimental points of ESR measured at 66 kHz and $T_a = 25$ °C, for aged capacitors at $T = 105$ °C.

An interpolation between these measured points gives the variation of ESR *versus* time for the aging at $T = 105$ °C. For any other aging temperature $T' \neq T$, another evolution law can be determined. In fact, as shows Figure 6, for every point (t, ESR) corresponding to the curve at $T = 105$ °C, the time t' corresponding to the temperature T' can be calculated by the Arrhenius law [8]:

$$\frac{t'}{t} = \exp\left(E\,\frac{T - T'}{TT'}\right) \tag{6}$$

where E is the activation energy divided by Boltzmann's constant. E is estimated to 4700 [12]. T and T' are the temperatures in Kelvin.

By considering $1/ESR$, a linear law [12,13] gives a theoretical prediction model of ESR *versus* time and temperature. It is given by the relation (7):

$$\frac{1}{ESR(t)} = \frac{1}{ESR(0)}\left[1 - kt\exp\left(-\frac{4\,700}{T}\right)\right] \tag{7}$$

where $ESR(t)$ is the ESR value at time $t \neq 0$. $ESR(0)$ is the ESR value at time $t = 0$. k is a constant depending on the construction and on the dimensions of the capacitor. t is the aging time. T is the aging temperature in Kelvin.

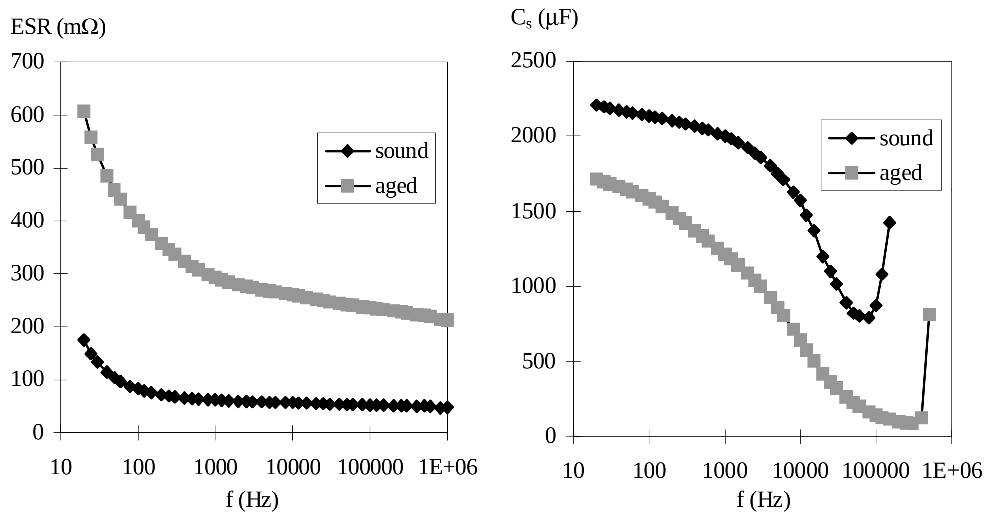

Fig. 5. Influence of the aging upon the characteristics of electrolytic capacitors.

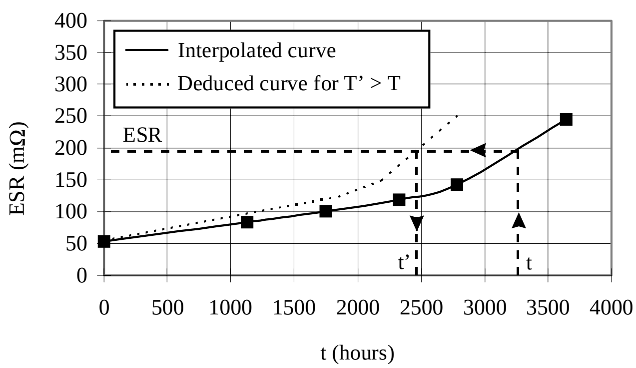

Fig. 6. Experimental model at 66 kHz fitting the aging law at $T = 105\,^{\circ}\mathrm{C}$.

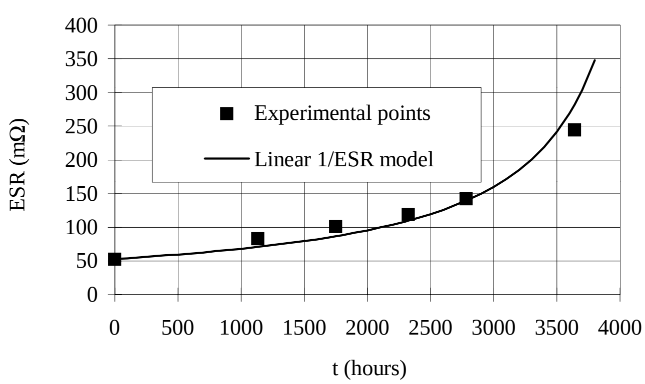

Fig. 7. Theoretical model at 66 kHz fitting the aging law at $T = 105\,^{\circ}\mathrm{C}$.

Figure 7 shows the theoretical law deduced from this model. The constant k is calculated by the least squares method to fit the experimental points ($k = 58$). This model is a little pessimistic but provides a simple representation of the capacitor behavior.

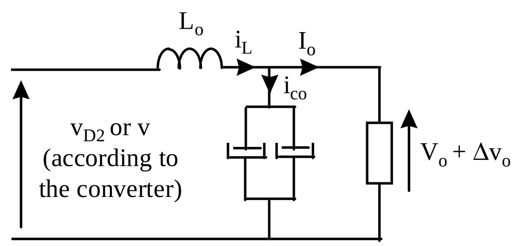

Fig. 8. Output circuit of the converters.

4 Electrical waveforms to monitor

4.1 Influence of electrolytic capacitors aging on the converters waveforms

4.1.1 Output capacitors of SC1 and SC2: Filtering function

The only signal that is significantly modified when the capacitors are aged, is the output voltage ripple of the latter. The changes occurring to the ripple signal could be explained as follows for the two converters (the output schema is similar for both (*cf.* Fig. 8); where V_o is the DC output voltage and Δv_o is the AC component at the switching frequency of the converters.

During operation of the converters, the output filter capacitors wear out similarly because they are stressed by the same current ripple and the same ambient temperature (they are mounted near on the converter). At the switching frequencies of the converters, the total impedance of each capacitor is almost equal to its ESR, then the global resistance ESR_{eq} of the equivalent capacitor is equal to $ESR/2$. The output voltage ripple Δv_o is linked to the ripple current i_{co} through the capacitors by:

$$\Delta v_o \approx ESR_{eq}\, i_{co}\,. \tag{8}$$

The current i_{co} is almost equal to the current ripple Δi_L through the output smoothing inductor L_o because the

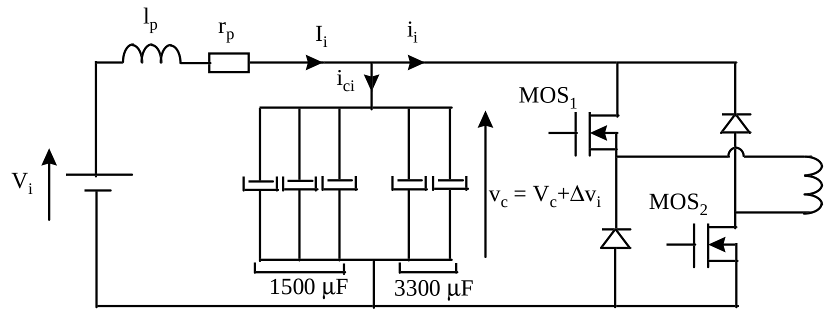

Fig. 9. Input circuit of the converter SC1.

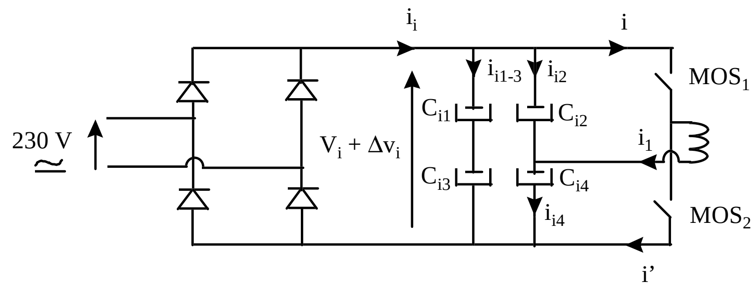

Fig. 10. Simplified input circuit of SC2.

load resistance (V_o/I_o) is much higher than the capacitors resistance ESR_{eq}. This ripple depends only on the parameters of the converters but not on the capacitors worn state [14,15].

Therefore, for given input voltage and output current, Δv_o increases with the aging of the capacitors as ESR_{eq} rises.

4.1.2 Input capacitors of SC1: Filtering function

Figure 9 illustrates the input circuit of SC1; r_p and l_p represent respectively the parasitic internal resistance and inductance of the batteries and the connecting wires.

At sound state, ESR of the capacitors rated 3 300 μF is equal to 22 mΩ and ESR of the capacitors rated 1 500 μF is 54 mΩ. The capacitors 3 300 μF have then a more rapid aging than the capacitors 1 500 μF. In fact, since $1/(C\omega) \ll ESR$, the Joule losses in the capacitors are given by:

$$P \approx \frac{(\Delta V_{i-eff})^2}{ESR} \tag{9}$$

where ΔV_{i-eff} is the RMS value of the input voltage ripple Δv_i. The external surface area of the 3 300 μF capacitors is 6 300 mm^2 and the surface area of the 1 500 μF capacitors is 4 200 mm^2. In addition, as the diameters of the 3 300 μF and 1 500 μF capacitors are identical and as the airflow conditions are approximately the same for the five capacitors (natural convection), H can be considered as a constant [9]. Then referring to equation (5) and equation (9) above, we conclude that the components rated 3 300 μF are stressed by a temperature difference ΔT almost 1.6 times higher than ΔT for the capacitors 1500 μF.

Concerning the filtering function, the study is similar to the output waveforms. The input voltage ripple Δv_i is linked to the current ripple i_{ci} through the input capacitors by the relation:

$$\Delta v_i \approx ESR_{eq}\, i_{ci} \tag{10}$$

where ESR_{eq} is the equivalent resistance of the five filter input capacitors.

The consequence of the wearout of the input capacitors is that Δv_i increases *versus* the resistance ESR_{eq}, since the ripple current i_{ci} is independent on the worn state of the capacitors [14].

The input capacitors does not wear similarly but only on ESR_{eq} influences Δv_i. The filtering function is affected by the aging of the equivalent capacitor. Then the monitoring of ESR_{eq} value is sufficient to determine the worn state of the capacitors.

4.1.3 Input capacitors of SC2: Filtering function

In Figure 10 is shown the equivalent input circuit of the converter SC2.

The capacitors C_{i1} and C_{i3} are used to filter the output voltage of the bridge rectifier whereas the capacitors C_{i2} and C_{i4} constitute the half bridge structure.

The input voltage can be divided into a low-frequency component V_i representing the rectified and filtered network source voltage and a high-frequency component Δv_i at a frequency equal to the double of the switching frequency of SC2 *i.e.* 150 kHz [14].

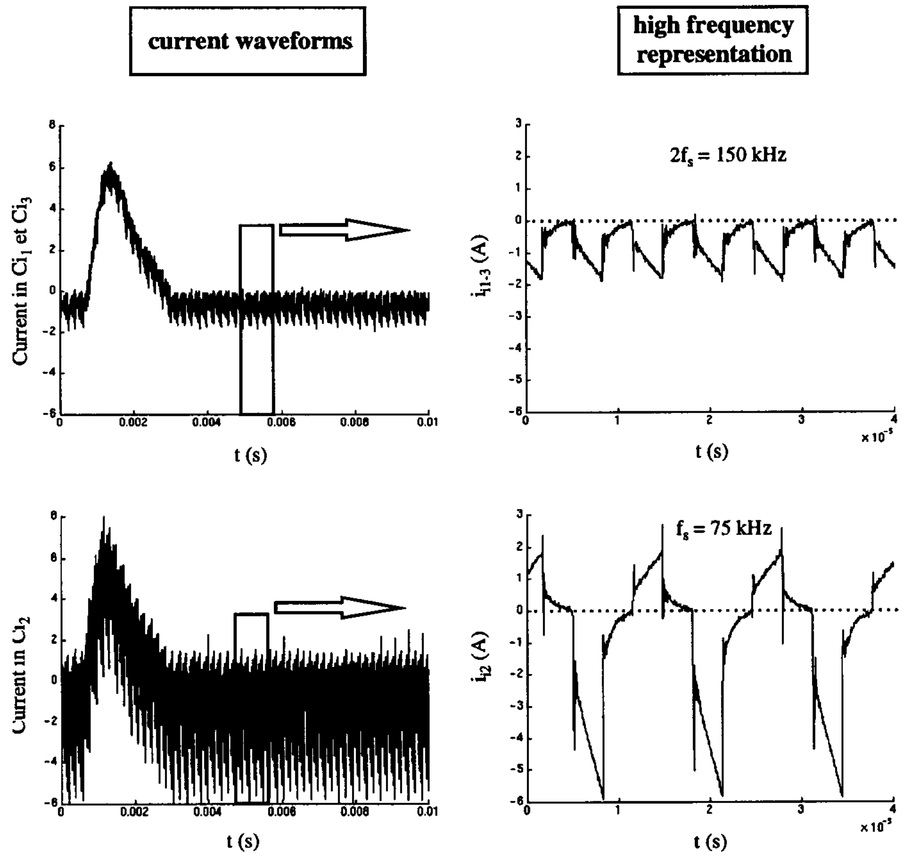

Fig. 12. Experimental current waveforms across the input capacitors.

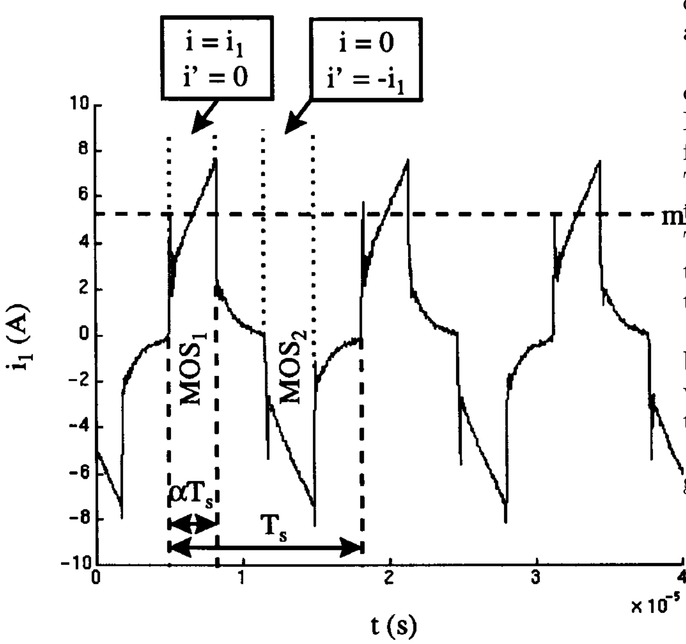

Fig. 11. Current i_1 in the primary circuit of the transformer for $I_o = 16$ A where α is the duty ratio and T_s is the switching period.

In Figure 11, we represent the current i_1 in the primary of the transformer measured experimentally for a running at $I_o = 16$ A.

The input capacitors are stressed by currents with different RMS values. Their aging is then not similar. In Figure 12, we show the different input current waveforms for the converter SC2 using sound input capacitors. The current $i_{i4}(t)$ through the capacitor C_{i4} is equal to the current i_{i2} through C_{i2} with a phase lagging of $T_s/2$. The RMS currents through C_{i2} and C_{i4} are greater than through C_{i1} and C_{i3}. Their aging is thus faster because the self heating is greater.

For high frequencies, the circuit of Figure 10 can be represented by the equivalent circuit of Figure 13a which can be transformed to Figure 13b by a Wye-Delta transformation (Fig. 13).

A simple expression of the input ripple voltage Δv_i is given by:

$$\Delta V_i(t) = \frac{ESR_{1-3}\,ESR_{2-4}}{ESR_{1-3} + ESR_{2-4}} \times (-i' - i) = -ESR_{eq}(i' + i). \quad (11)$$

When input capacitors wear, the input ripple voltage Δv_i increases proportionally to ESR_{eq}. The currents i and i' can be considered as independent of the worn state of the capacitors [14].

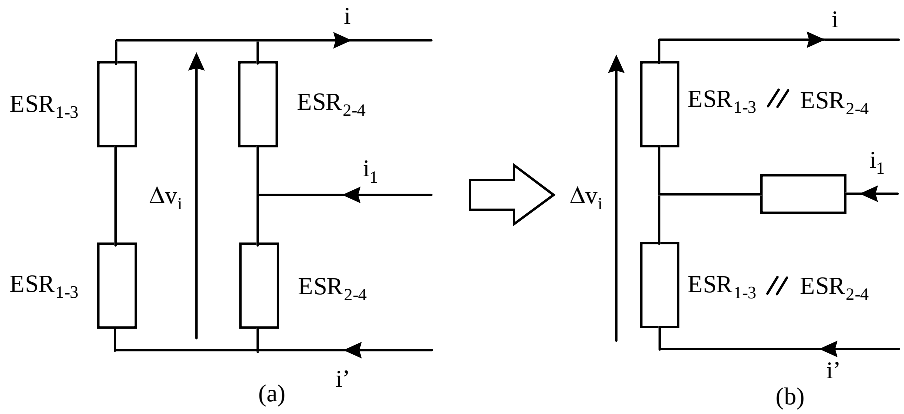

Fig. 13. Wye - Delta transformation of the input circuit of SC2.

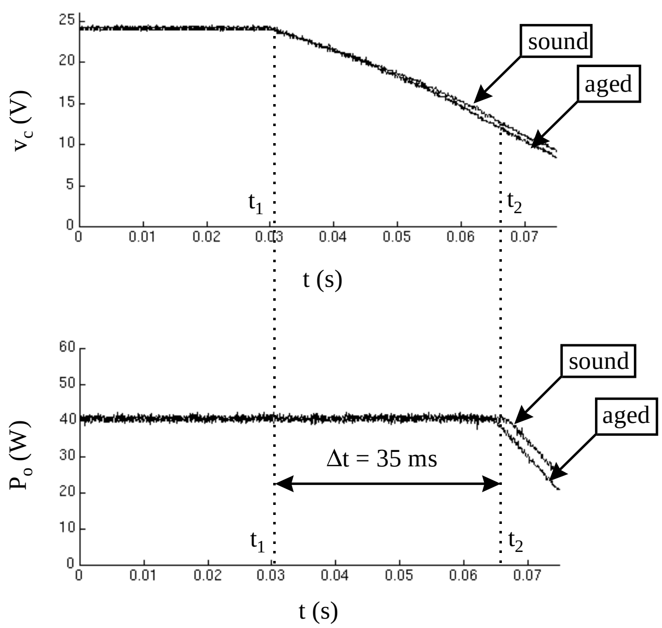

Fig. 14. Output power transfer for a switching operation of input batteries.

4.1.4 Input capacitors of SC1: Energy storage function

The input batteries of the converter SC1 deliver a DC voltage. The discharge of these batteries makes the DC voltage drops. Thus, they must be changed. The industrial requirements specify that when batteries are switched, the input capacitors must deliver electrical energy during at least 20 ms.

The purpose is to show the influence of the capacitors aging on the input voltage and on the output power transmitted to the load.

For sound input capacitors (ESR_{eq} = 17 mΩ, C_{eq} = 10.5 mF at 25 ℃ and 20 Hz) and worn capacitors (ESR_{eq} = 38.7 mΩ, C_{eq} = 10 mF at 25 ℃ and 20 Hz), Figure 14 illustrates the voltage v_c measured across the terminals of the capacitors and the output power $P_o = V_o I_o$ during a switching operation of the input batteries.

Between the switching instant (t_1) and the instant when the output power P_o drops (t_2), the input capacitors supply energy to the converter, the power P_o is maintained constant during a period Δt of about 35 ms which responds to the requirements.

Besides, we note that the voltage v_c and the power P_o are not much affected by the capacitors wearout. This can be argued by two reasons:

– At first, for low frequencies, the capacitance of an electrolytic capacitor is the preponderant element of its impedance: for the five input capacitors of SC1, the global capacitance C_{eq} decrease is equal to 5% while ESR_{eq} increases about 100%.

– Secondly, the equivalent resistance of the global circuit below the input capacitors (equal to V_i/I_i) is much greater than ESR_{eq}.

4.2 Transient state due to load variation

To monitor the state of filter electrolytic capacitors, some authors [3,4] take into account the whole ripple voltage across the capacitors. This method present a major disadvantage, it can not be applied to static converter working at variable load.

The aim of this paragraph is to show the influence of an output current variation on input and output voltage ripples Δv_i and Δv_o for the converters SC1 and SC2.

4.2.1 Influence of a load variation on Δv_o

We have subjected the converters SC1 and SC2 to a load variation as shown in Figure 15 and measured experimentally the voltage ripple Δv_o.

We observe a transient increase of Δv_o when the output current changes.

4.2.2 Theoretical interpretation of the results

Let us explain this transient phenomenon. The output circuit of the converters SC1 and SC2 is represented in Figure 16.

The voltage denoted by u represents v_{D2} in the case of SC1 and v in the case of SC2 (*cf.* Fig. 8).

The output circuit of the converters can be considered as a superposition of low and high frequency circuits.

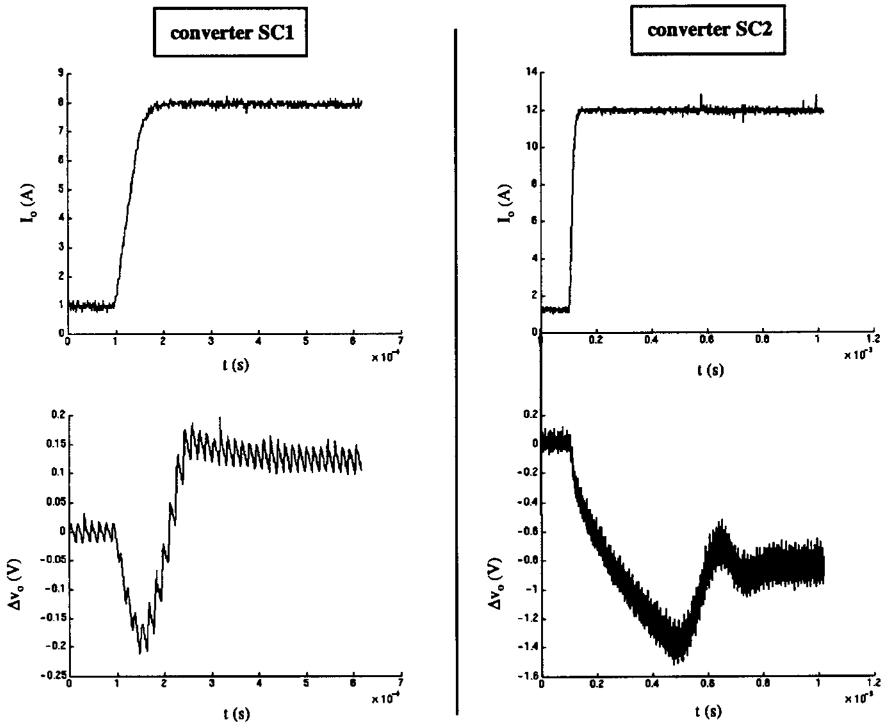

Fig. 15. Influence of a variable load on Δv_o.

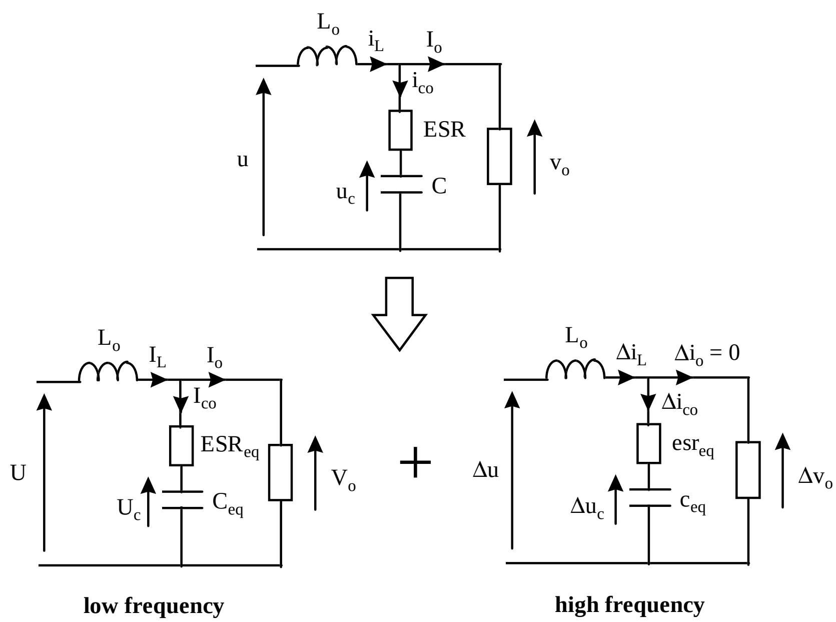

Fig. 16. Output circuit of SC1 and SC2.

All the input waveforms are then divided into low-frequency and high- frequency components:

$$
\begin{aligned}
u &= U + \Delta u \\
v_o &= V_o + \Delta v_o \\
i_{co} &= I_{co} + \Delta i_{co} \\
i_L &= I_L + \Delta i_L \\
u_c &= U_c + \Delta u_c. \qquad (12)
\end{aligned}
$$

For the low frequencies, the input waveforms are given by:

$$U = ESR_{eq} I_{co} + U_c + L_o \frac{dI_L}{dt} \qquad (13)$$

$$I_{co} = C_{eq} \frac{dU_c}{dt} \qquad (14)$$

$$I_L = I_o + I_{co} \qquad (15)$$

$$V_o = ESR_{eq} I_{co} + U_c. \qquad (16)$$

At steady state operation, the input signals are expressed as follows:

$$\begin{aligned} I_{co} &= 0 \\ I_L &= I_o = Constant \\ U &= V_o = U_c. \end{aligned} \quad (17)$$

When the converter works at a transient operating mode, the current I_{co} through the output capacitors is no more equal to zero.

The parameters of the capacitors (ESR_{eq}, C_{eq}) are calculated at low-frequency. This frequency (f_{eq}) is determined according to the load variation waveform [14].

We suppose that f_{eq} is always less than 1/10 of the switching frequency of the converter to make possible the separation between low and high-frequency components.

By denoting m the transformation ratio between the primary and the secondary of the transformer, α the duty ratio of the converter, the average value $\langle u \rangle$ of the voltage u is function of V_o and V_i:

$$\langle u \rangle = \alpha m V_i \quad (18)$$

$$\langle u \rangle = V_o. \quad (19)$$

In transient mode, the relation (19) is no more right, because the current I_o is variable, the current in the inductor L_o is not constant. To simplify the study, we can suppose $\langle u \rangle$ still equals $\alpha m V_i$ because α and V_i remain unchanged. As $\langle u \rangle = U$ (high-frequency component Δu has a mean value equal to zero), we consider that U remains constant (equal to 5 V in the case of SC1 and 24 V in the case of SC2). Equations (13), (14) and (15) give:

$$U = U_c + ESR_{eq} C_{eq} \frac{dU_c}{dt} + L_o \frac{d}{dt}\left(I_o + C_{eq}\frac{dU_c}{dt}\right) \quad (20)$$

then:

$$U_c + ESR_{eq} C_{eq} \frac{dU_c}{dt} + L_o C_{eq} \frac{d^2 U_c}{dt^2} = U - L_o \frac{dI_o}{dt} \cdot \quad (21)$$

Referring to the equations (14) and (16), the output voltage V_o can be written as:

$$V_o = U_c + ESR_{eq} C_{eq} \frac{dU_c}{dt} \cdot \quad (22)$$

If we denote by V_{excit} the voltage $U - L_o \frac{dI_o}{dt}$, we have:

$$\frac{V_o(p)}{V_{excit}(p)} = \frac{\omega_o^2 + 2z\omega_o p}{p^2 + 2z\omega_o p + \omega_o^2} \quad (23)$$

where p: Laplace operator

$$z = \frac{ESR_{eq}}{2}\sqrt{\frac{C_{eq}}{L_o}}$$

$$\omega_o = \frac{1}{\sqrt{L_o C_{eq}}} \cdot$$

We represent in Figure 17 the output voltage V_o response to the excitation voltage V_{excit}, for a variable current I_o.

In Figure 17 the transient phenomenon at low-frequency of the output voltage can be seen quite similar to the measured one (Fig. 15).

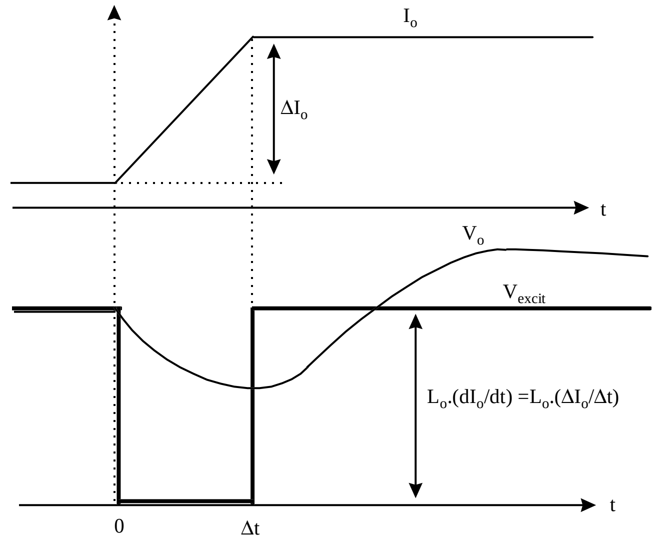

Fig. 17. Theoretical interpretation of the transient of the V_o voltage.

4.2.3 Parameters to monitor

In order to avoid errors in the lecture of the state of the filtering capacitors, the increase of the transient values of Δv_o should not be a synonym of ESR rise.

To overcome such problem, we chose as indicator of fault of the capacitors, the fundamental component Δv_{of} of the voltage ripple Δv_o.

The choice of the average rectified signal of Δv_o as fault indicator, suggested by some authors [3,4], gives the same results as Δv_{of} in steady state operation only, but does not avoid the transient values of Δv_o and may generate wrong predicted service life of the capacitors.

To facilitate the processing of the different waveforms [1,14], the signal considered to monitor the ESR value, is the average rectified signal of Δv_{of}.

We represent in Figure 18, the fundamental signal Δv_{of} (Curve 1a for SC1 and Curve 2a for SC2), the average rectified signal of Δv_{of} (Curve 1b for SC1 and Curve 2b for SC2) and the average rectified value of the original signal Δv_o (Curve 1c for SC1 and Curve 2c for SC2) for a load variation sequence. We notice that the surge value of Δv_o is completely detected by the Curves 1c and 2c while the Curves 1b and 2b show a negligible increase of the image of Δv_o considered. Because of the high transient values affecting the Curves 1c and 2c, they can not be used as indicators of fault of the capacitors. The Curves 1b and 2b show a little increase at the moment of the load change and give a faithful image of the capacitors worn state.

4.2.4 Influence of the aging on Δv_o at variable load

We have shown the influence of the aging of filtering capacitors on converters waveforms in steady state operation, we observe now their influence in variable load operation.

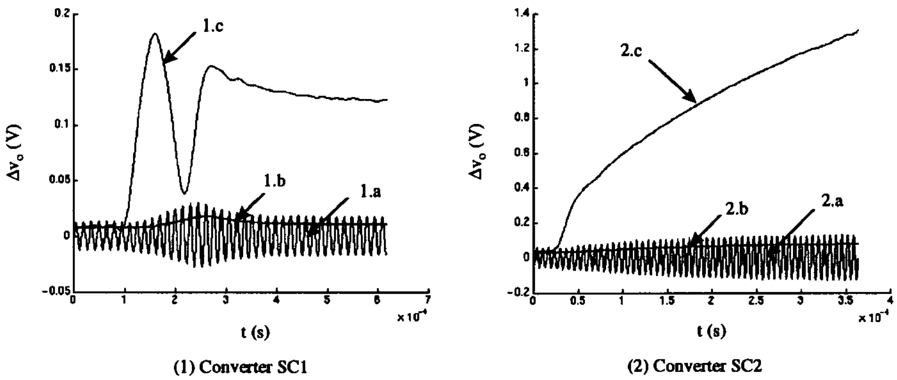

Fig. 18. Processing of Δv_o.

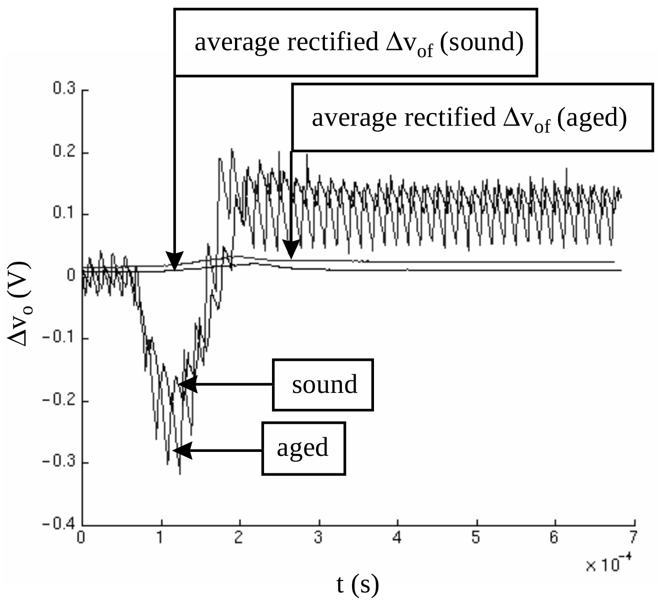

Fig. 19. Transient of Δv_o for sound and aged capacitors.

For example, Figure 19 illustrates the voltage ripple Δv_o of SC1, for the load variation of Figure 15, with sound capacitors (ESR_{eq} = 27 mΩ at 25 °C and 66 kHz) and worn capacitors (ESR_{eq} = 71 mΩ at 25 °C and 66 kHz).

We observe that the aging of the capacitors affects Δv_o in steady state operation and at variable load operation by inducing higher transient values of Δv_o. The average rectified signal of Δv_{of} shows a negligible increase and provides better image worn state of the capacitors.

4.2.5 Influence of the load variation on Δv_i

We studied the input voltage ripple for a load variation sequence. For the two converters SC1 and SC2, we have detected transient values of Δv_i due to the variation of Δv_o (*cf.* Fig. 20).

For the converter SC2, the low-frequency component of the input voltage is also affected by the load change.

Similarly as for the output voltage, Figure 20 confirms the necessity to consider the fundamental component Δv_{if} of the ripple voltage Δv_i. In fact, this signal shows a negligible increase under a load change and gives a satisfying image of the worn state of the input filter capacitors.

5 Prediction method of the capacitors Fault

We demonstrated in Section 3 that the electrolytic capacitors wearout depends on aging time and temperature applied to the components. Their electrical characteristics drift and especially the equivalent series resistance ESR increases.

For the industrial users of switched power supplies, the definition of the capacitors useful working life is fixed by the voltage ripple admitted. For the converters SC1 and SC2, the limit voltage ripples Δv_{if} and Δv_{of} define the limit value of ESR and then the useful life of the capacitor [16].

The aim of the study is to utilize the voltage ripple to determine the ESR value of filter electrolytic capacitors at any time t, for given temperature T_a, current I_o and voltage V_i. A prediction model of ESR is used then to predict the time remaining to failure.

For the input and the output circuits of the converters, the average rectified value (δV_f) of the fundamental voltage ripple (Δv), is function of the resistance ESR_{eq} but also on the output current I_o and the input voltage V_i. We get then:

$$\delta V_f = f(I_o, V_i, ESR_{eq}). \tag{24}$$

As shown previously (*cf.* Sects. 4.1.1, 4.1.2, and 4.1.3), ESR_{eq} is function of the ESR values ESR_1 and ESR_2 of each filter capacitor and can be written as:

$$ESR_{eq} = f(ESR_1, ESR_2). \tag{25}$$

For sound capacitors, we determine experimentally the function $\delta V_f = f(ESR_{eq})$ for I_o and V_i given.

The resistance ESR_1 and ESR_2 are function of the case temperatures T_{c1} and T_{c2} of each capacitor (*cf.* Fig. 4). ESR_1 and ESR_2 can be written as follows:

$$ESR_1 = f(T_{c1}) \tag{26}$$

$$ESR_2 = f(T_{c2}) \tag{27}$$

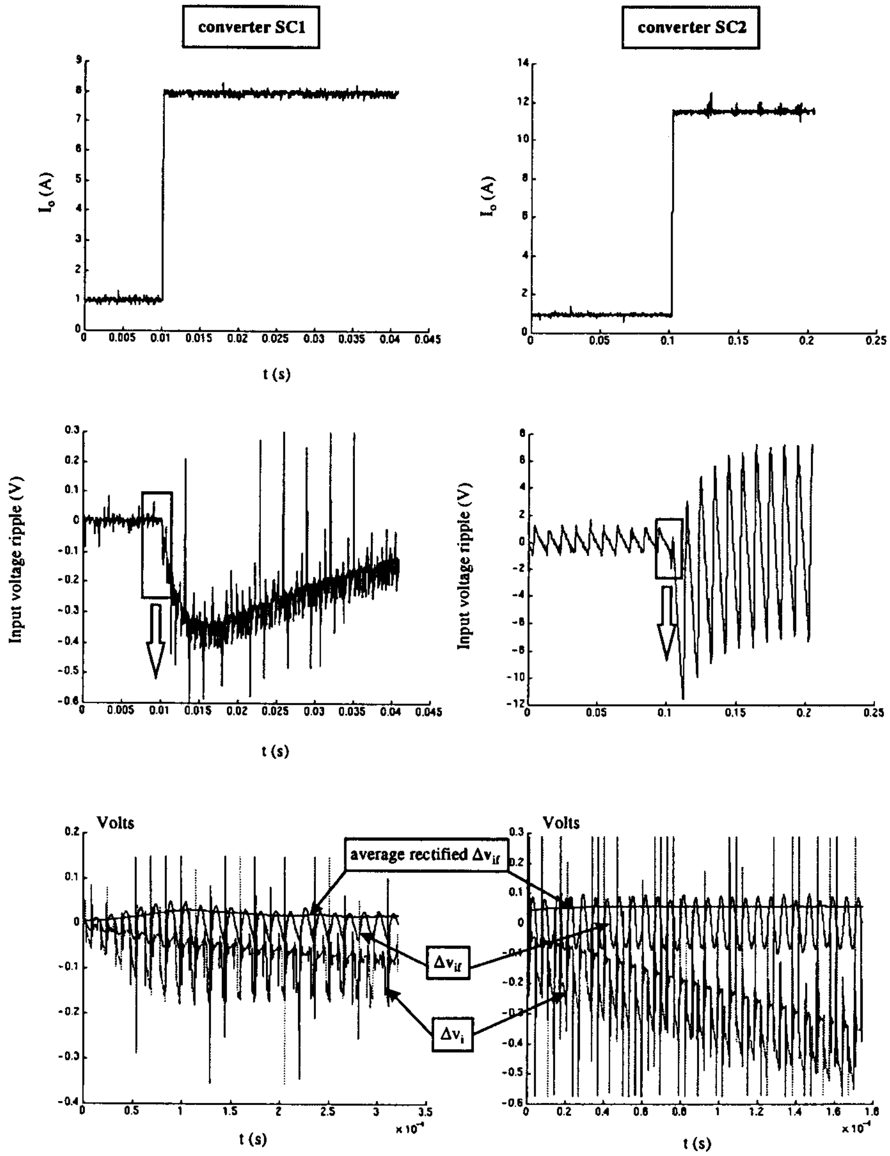

Fig. 20. Processing of Δv_i.

Referring to equations (4) and (5), for a given resistance ESR, the case temperature T_c is a function of the ambient temperature T_a and of the RMS value of the ripple current through the capacitor. This latter depends on I_o and V_i, then:

$$T_{c1} = f(I_o, V_i, T_a) \tag{28}$$

$$T_{c2} = f(I_o, V_i, T_a). \tag{29}$$

Equations (25) to (29) give:

$$ESR_{eq} = f(I_o, V_i, T_a). \tag{30}$$

The relation (24) becomes:

$$\delta V_f = f(I_o, V_i, T_a). \tag{31}$$

For sound capacitors, knowing the values of δV_f, I_o and V_i, the relation (31) gives the ambient temperature T_a. The temperatures T_{c1} and T_{c2} are then calculated from the equations (28) and (29). The ESR_1 and ESR_2 values are deduced from the equations (26) and (27). The function $\delta V_f = f(ESR_{eq})$ is thus experimentally determined. The method established is summarized in Figure 21.

When capacitors wear under aging conditions, the function $\delta V_f = f(ESR_{eq})$ is unchanged because it does not depend on the worn state of the capacitors but only on the ripple current *i.e.* I_o and V_i (*cf.* Eqs. (8), (10) and (11)).

The knowledge of δV_f, I_o and V_i is sufficient at any time of the capacitors life, to compute the value of ESR_{eq} as illustrated in Figure 21.

Hence, the predictive maintenance method needs two essential parts:

- The measurement at $t = 0$, for the converter using sound electrolytic filter capacitors of the signals δV_f,

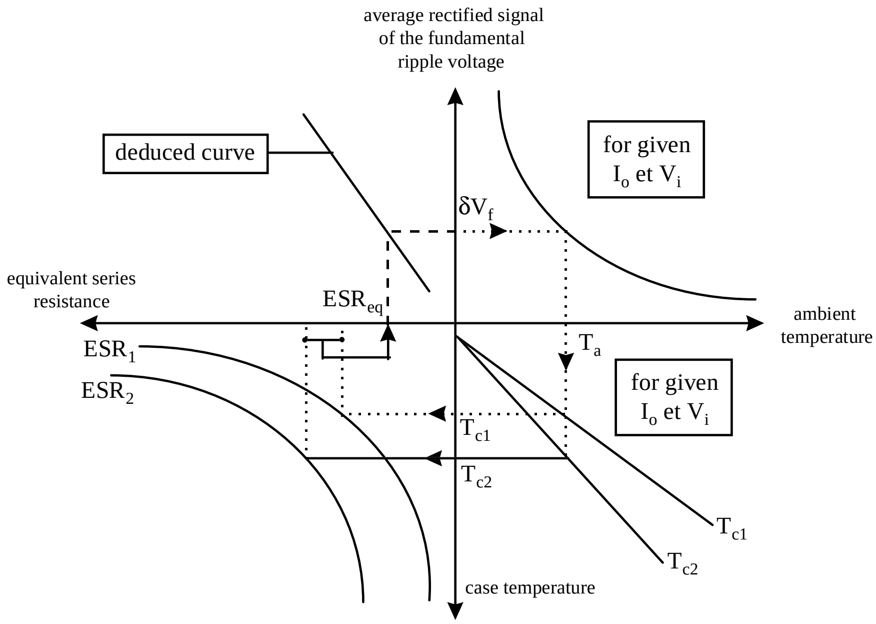

Fig. 21. Monitoring method of the filter electrolytic capacitors.

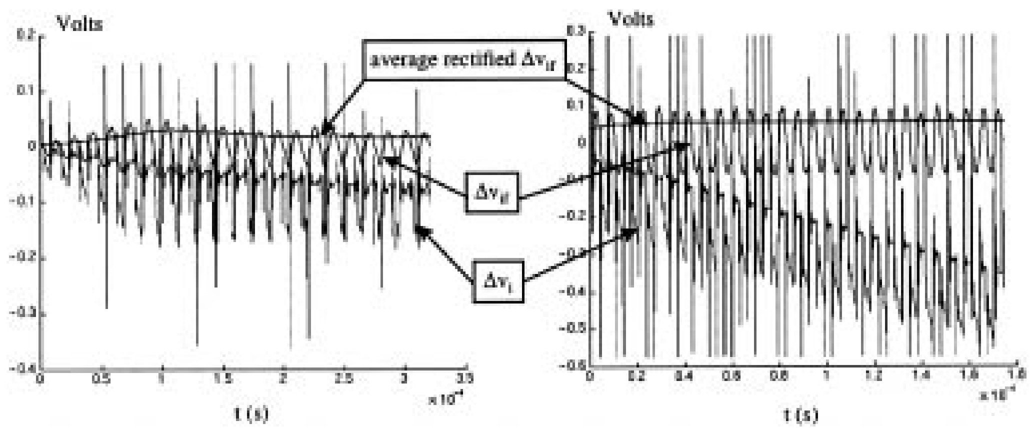

Fig. 22. Results obtained with sound and worn capacitors for $I_o = 8$ A, $V_i = 24$ V and $T_a = 25\,°$C.

T_{c1}, T_{c2}, I_o, V_i and T_a and the storage of the functions δV_f, T_{c1} and T_{c2} *versus* I_o, V_i and T_a (*cf.* relations (28), (29) and (31)).

- The measurement at $t \neq 0$, during operation of the converter, of the signals:
  - δV_f, I_o, V_i in order to deduce the value of ESR_{eq} at that time.
  - The temperature T_a that gives the case temperature of each capacitor and then ESR_{eq} for sound capacitors [14].

A prediction model of ESR_{eq} *versus* time and temperature is finally used to compute the time remaining to failure (*cf.* Eq. (7)).

6 Results

Figure 22 shows the results obtained by the fault prediction method of capacitors, applied to the output circuit of the converter SC1, using sound components (Fig. 22a) and aged components (Fig. 22b). We can see how an aged capacitor reduces to 2.5 years the time before failure of the converter.

7 Conclusion

Accelerated aging tests carried out on electrolytic capacitors showed that the equivalent series resistance ESR is the best indicator of fault of these components. ESR increases according to a well known law *versus* aging time and temperature.

We also observed the influence of the aging of the capacitors on the voltage filtering and proved that in steady state operation, the voltage ripple increases almost proportionally to ESR.

At variable load state, we found that high transient values occurred on the voltage ripple which can lead to faulty alarms by giving wrong predicted values of the resistance ESR. To avoid such errors, we suggest the monitoring of the fundamental component of the voltage ripples.

We noted too that the storage function of electrical energy is almost unaffected by the aging of capacitors.

Since the voltage ripple depends on ESR and also on the output current, the input voltage and the ambient temperature, all these parameters are taken into account in the fault prediction method.

The results obtained by this method were confirmed by industrial users.

Authors would like to thank CENTRALP- AUTOMATISMES and ANVAR for their technical and financial contribution in this work.

References

1. P. Venet, *Surveillance d'alimentation à découpage. Application à la maintenance prédictive*, Ph.D. thesis, Université Claude Bernard, Lyon, 1993.
2. A. Lahyani, P. Venet, G. Grellet, P.J. Viverge, IEEE Trans. Power Electr. **13**, 6, 1199 (1998).
3. K. Harada, A. Katsuki, M. Fujiwara, IEEE Trans. Power Electr. **8**, 4, 355 (1993).
4. K. Harada, Pat. Jpn **12**, 313, (1988).
5. P. Venet, A. Lahyani, P.J. Viverge, G. Grellet, EPE'97 Proc. **2**, 978 (1997).
6. P. Venet, H. Darnand, G. Grellet, INTELEC'93 Proc. **2**, 229 (1993).
7. B. Alvsten, *Electrolytic capacitors theory and application* (RIFA Electrolytic Capacitors, Sweden, 1995).
8. M.L. Gasperi, IEEE IAS Conference Proc. 1347, (1996).
9. H. Michel, Siemens Components **27**, 5 33 (1992).
10. S. Andoh, T. Itoh, T. Shimpo, Y. Yokoyama, INTELEC'86 Proc. 479 (1986).
11. E. Marchese, Power Techn. **6**, 12 (1984).
12. G.E. Rhoades, A.W.H. Smith, 34th Component Conference Proc. 156 (1984).
13. J.A. Jones, Hayes, *The parametric drift behaviour of aluminium electrolytic capacitors: An evaluation of four models*, 1st European Capacitor and Resistor Technology Proc. p. 171 Brighton 1987.
14. A. Lahyani, *Surveillance et diagnostic d'état des condensateurs électrolytiques dans les convertisseurs statiques*, Ph.D. Thesis, Claude Bernard University, Lyon, 1998.
15. J.P. Ferrieux, F. Forest, *Alimentations à découpage, convertisseurs à résonance, principes,composants, modélisation*, (Masson, Paris, 1994).
16. P. Venet, A. Lahyani, G. Grellet, *Procédé et dispositif pour déterminer l'état de vieillissement d'un condensateur*, Pat. France **97**, 335 (1997).